THE LBL 88-INCH CYCLOTRON OPERATING WITH AN ECR SOURCE

Clark, D. J.

1986-10-01

LBL-22715

Lawrence Berkeley Laboratory
UNIVERSITY OF CALIFORNIA

Presented at the 10th National Conference
on Particle Accelerators,
Dubna, U.S.S.R., October 21–23, 1986

# THE LBL 88-INCH CYCLOTRON OPERATING WITH AN ECR SOURCE

D.J. Clark

October 1986

NUCLEAR SCIENCE DIVISION

Prepared for the U.S. Department of Energy under Contract DE-AC03-76SF00098

LBL 22715

# THE LBL 88-INCH CYCLOTRON OPERATING WITH AN ECR SOURCE*

David J. Clark
Lawrence Berkeley Laboratory, University of California
1 Cyclotron Road, Berkeley, CA 94720, U.S.A.

*This work was supported by the Director, Office of Energy Research, Division of Nuclear Physics of the Office of High Energy and Nuclear Physics and by Nuclear Sciences of the Basic Energy Sciences Program of the U.S. Department of Energy under Contract DE ACO3-76SF00098.

# THE LBL 88-INCH CYCLOTRON OPERATING WITH AN ECR SOURCE

David J. Clark
Lawrence Berkeley Laboratory, University of California
1 Cyclotron Road, Berkeley, CA 94720, U.S.A.

## Introduction

The LBL 88-Inch Cyclotron is a variable energy, multi-particle sector-focused cyclotron which has been operating since 1962. It provides a wide variety of light and heavy ion beams for nuclear science and solid state physics research. The layout of the experimental cave areas is shown in Fig. 1. High intensity beams of 5-20 μA are run in Caves 0 and 3 for isotope production and transuranic research. High intensity beams are also used in Cave 2 for the production of exotic nuclei far from the region of stability, with the help of an on-line mass analyzer. In Cave 5 research on high spin states of nuclei is carried out with a gamma ray ball detector. The two 110 degree analyzing magnets give high resolution beams which are used for heavy ion reactions in Cave 4A or 4C. A scattering chamber in Cave 4B is available for polarized beam experiments with protons and deuterons. A new gamma ray detector has also been installed in Cave 4C.

A layout of the cyclotron acceleration region is shown in Fig. 2. Both internal and external ion sources are used. The design includes a 3 sector magnetic field and a single 180 degree dee. The rf voltage is up to 50 kV and the frequency is 5.6 to 16.6 MHz. 100% duty factor is used for the rf and the ion source. A resonance chart is shown in Fig. 3, indicating the charge/mass ratios of the various ions which can run on the first and third harmonic mode. The dots indicate points where complete running parameters have been calculated. Other particles and energies can be run using the appropriate data from the nearest calculated point. Protons are normally accelerated up to 55 MeV, deuterons to 65 MeV, $^3$He to 140 MeV, alpha-particles to 130 MeV and heavier ions as high as K=160, but usually only up to K=140. Here K is the cyclotron energy constant defined by $E=KQ^2/A$; E is cyclotron energy (MeV); Q and A are particle charge and mass. A polarized ion source is used with an axial injection system for beams of polarized protons and deuterons. In Fig. 4 the contours indicate beam intensities on a E/A vs. A plot. The "PRESENT 88" curves show the heavy ion beam intensities available with the PIG source up to 1984. In 1985 the ECR source and injection line came into regular operation and gave the increase in intensity and energy shown in the higher set of curves in Fig. 4. The ECR source is used for about 80% of the cyclotron operating time. During the remaining 20% of the time light ion beams are produced by the filament source and polarized protons and deuterons by the polarized ion source.

## The ECR Source

The main features of the ECR source are illustrated in Fig. 5. Many features have been described previously/1-5/. It has two stages. In the first stage the plasma is created by feeding microwave power and gas at about $10^{-3}$ torr into a tube containing an ECR resonance. Ions drifting from the first stage to the second stage are ionized step by step by fast electrons trapped by the mirror field in the second stage ECR resonance zone region. Here the pressure is much lower than in the first stage, about $10^{-6}$ torr, to minimize recombination of the high charge state ions. The first stage uses a 1 kW 9.2 GHz klystron (typical power 100 W) and the second stage uses a 3 kW 6.4 GHz klystron (typical power 400 W). The axial magnetic field is produced by tape wound edge cooled copper coils each powered by an individual supply for maximum flexibility in magnetic field configuration. Typical magnet power is 30 kW. The radial magnetic field is produced by a $SmCo_5$ sextupole with slots which allow radial pumping. Pumping is done by diffusion pumps. The extraction system is accel-decel to provide a high voltage across the extraction gap and reflect neutralizing electrons from the transport system.

The performance of the ECR source is summarized in Tables 1 and 2. The source was tuned for a high charge state in most cases. Beams such as nitrogen, oxygen and argon are well optimized. Beam voltage is 10 kV and duty factor is 100%. Larger currents can be obtained at higher extraction voltage. For example, the current for $Ar^{8+}$ increased from 106 μA at 10 kV to 140 μA at 14 kV.

Gases are easy to run in the source. They can be mixed and can be fed into either the first stage, second stage or both stages. For high intensity proton and alpha beams gas is fed directly into the second stage and the first stage is turned off. For all elements heavier than oxygen, a lighter gas is added to enhance the high charge state performance of the source. The presence of heavy ions in the plasma also acts to depress the charge state performance of light ions. A charge state distribution for oxygen measured on the LBL ECR is shown in Fig. 6. Beams of carbon, sulfur and silicon are produced from the gaseous compounds $CH_4$, $SO_2$ and $SiH_4$ respectively. They are injected into the second stage to avoid contamination of the first stage due to the high flow rates required there. Metallic ion beams are produced using a resistance heated oven inserted radially into the second stage. Vaporized metal ions are ionized by the plasma. A temperature controller keeps the oven temperature constant. Cyclotron runs lasting several days have used metal ion beams with little or no adjustment to the source or oven. For a potassium beam the oven was loaded with a mixture of KCl and Ca and heated. Calcium reacts with KCl forming $CaCl_2$ and potassium vapor. This technique avoided the problems of handling potassium metal and reduced the chlorine beam intensity. For beams from high temperature materials such as Al, Fe, Ti and Nb a rod has been inserted into the 2nd stage plasma. To use this method for routine cyclotron operation feedback would have to be used to control rod position or rf power.

The ECR source runs for many days without any maintenance, while the PIG source required cathode changes at 2-8 hour intervals running at the usual 100% duty factor. So with the ECR source the beam on target time is increased and manpower needed for source maintenance is reduced.

## The Injection System

The injection system/1-6/ for the Cyclotron ECR Source consists of 7 meters of horizontal beam line following the ECR source analyzing magnet, and 4 meters of vertical beam line down the axis of the cyclotron. Magnetic rather than electrostatic bending, focusing and steering elements were chosen because of better space charge neutralization, fewer vacuum penetrations and better long term reliability. Focusing is done with quadrupoles and Glaser lenses (magnetic solenoids with iron return yokes). Coils mounted on the beam pipe provide steering. To minimize beam steering due to the stray field of the cyclotron, nickel plated magnetic steel beam pipes were used where possible. The vacuum system uses cryo-pumps and turbo-pumps and all metal seals. The typical beam line pressure is $5 \times 10^{-8}$ Torr which is sufficiently low so that beam loss due to charge exchange with residual gas is negligible. Beam diagnostics along the injection beam line consist of fixed four jaw collimators with beam readouts before each set of lenses where the beam is large. Beam current can be read on several Faraday cups along the line.

A beam envelope calculation through the entire injection line is shown in Fig. 7. The horizontal beam line is shown in Fig. 8. The ECR source beam is focused by the first Glaser lens through the first slit on to the first Faraday cup. The beam is then analyzed and refocused by the 90 degree magnet through a second slit onto a 2nd Faraday cup. A resolution of about 1/100 in mass is obtained with 0.8 cm wide slits. Since the energy spread of the ECR beam is less than 1/1000, the dispersion contribution to the beam size is negligible. Just after the first quadrupole doublet there is a scanning Faraday cup which can be used to scan across the beam with the quadrupole off, and measure emittance. The emittance of the central core of the beam ranges from 20-110 $\pi$ mm mrad at 10 kV, un-normalized, going from high to low charge states. The energy spread of the central core is .1-5 eV for high to low charge states. The beam is transported by two magnetic quadrupole doublets to the 15 degree and 75 degree magnets which bend it into the vertical line, shown in Fig. 9. The polarized ion source is mounted vertically above the axial injection line and is used to inject polarized protons and deuterons. In the vertical line the focusing elements are 3 Glaser lenses. The bottom Glaser lens is placed at the bottom of the axial hole in the cyclotron yoke. It uses the cyclotron yoke as the magnetic return path. The computer program Poisson was used to calculate the Glaser magnetic field at high and low cyclotron fields.

A gridded buncher is placed 2.1 m above the cyclotron midplane. It consists of an electrode driven at cyclotron rf frequency with a typical voltage of several hundred volts. The grids are placed on the entrance and exit of the electrode and on the ground electrodes facing the entrance and exit. Fig. 10 shows the relation between the buncher voltage, $V_B$, the beam injection voltage, $V_i$, the particle charge state, Q, the cyclotron harmonic number, H, and the cyclotron beam energy, $E_C$. The beam travels about half an rf cycle in the electrode, so the effective length of the electrode, $L_B$, is about 1/2 $\beta\lambda$, where $\beta$ is v/c and $\lambda$ is rf wavelength. The system covers a broad cyclotron energy range as shown by the $E_C/A$ scales set in the upper part of Fig. 10 for ions with charge/mass Q/A = .5 and .25. At the bottom of the hole the beam enters the cyclotron magnetic field shown in Fig. 11. This field produces a strong focusing effect on the beam[1].

## The Center Region

At the median plane the beam is bent through 90 degrees by a gridded electrostatic mirror, shown in Fig. 12. The voltage on the mirror is typically .7 times the beam voltage. The wires are .005 cm diameter tungsten at .1 cm spacing. So the transmission of the beam in and out of the grid is 90%. Beam current can be read on the mirror with the voltage off. After leaving the mirror the beam enters the cyclotron center region, shown in Fig. 13. Inserts are placed in the dee and dummy dee to form narrow gaps for efficient acceleration. In our non-scaling mode of operation the orbits in this geometry do not have to have a constant pattern. This is indicated in Fig. 13 with a high and low energy beam. The requirement for beam centering is that the dee voltage should be approximately 5 times the injection voltage. The usual operating values are 10 kV for the injection voltage and 50 kV for the dee voltage. The advantage of operating in this non-scaling mode is that the dee voltage can be operated near its maximum for all beams, giving the minimum number of particle turns and thus high center region acceptance and low beam loss due to stripping during acceleration. Also, keeping the injection voltage high reduces the emittance in the transport line, giving higher transmission. The electric potential in the center region was calculated with the RELAX-3D program from the TRIUMF Cyclotron group. The central orbits were then calculated both in the median plane and with axial motion with the TRIWHEEL program from TRIUMF.

## Accelerated Beams

The cyclotron has accelerated many beams using this injection system. Some of the well tuned beams are shown in Table 3. The best transmission of 17% is found for the medium K range of K=80-100, near the low frequency end of the 1st harmonic mode. This is the region of low turn number where the center region acceptance is greatest. It is fortunate that this region includes beams such as $^{18}$O and $^{22}$Ne near the Coulomb barrier of 5 MeV/u where high intensities are often needed. The center region acceptance drops off at high turn number beams such as 429 MeV $^{16}O^{7+}$. 3rd harmonic beams are run frequently with good transmission of 10% for medium K beams such as $^{40}Ar^{9+}$. 5th harmonic has been tested, but the center region acceptance drops much below that of 3rd harmonic, and transmission is only 0.2%. 7th harmonic has also been tested and showed a further large drop in transmission. The 5th and 7th harmonic beams have not been requested for runs because of their very low energy, and would require a center region modification to run efficiently. The loss of beam due to charge exchange during acceleration ranges from 10% for highly stripped light ions to over 50% for heavy ions such as xenon.

A set of well tuned beams spanning the 1st and 3rd harmonic operating range was analyzed to understand the systematics of the many parameters which are tuned in the injection line and cyclotron to optimize the external cyclotron beam. Using the theoretical relation between parameters as a guide, a program was written to predict these parameters. For new beams these settings normally produce beam quickly on the internal cyclotron probe and then on the external Faraday cup. The parameters are then tuned for maximum transmission.

## Summary

The new ECR source and injection system have greatly expanded the range of particles and energies available from the LBL 88-Inch Cyclotron. The external beam intensities are adequate for experimental needs, ranging from 100 nA for 27 MeV/u oxygen to 5-10 μA for 6 MeV/u oxygen and neon. The lifetime of the source is days or weeks compared to hours for the PIG source, resulting in increased beam-on-target time and reduced manpower required for maintenance. Future possible improvements include the installation of higher frequency rf power for the ECR source 2nd stage to increase the high charge state output.

## References

1. D. J. Clark, J. G. Kalnins and C. M. Lyneis, IEEE Trans. on Nucl. Sci. NS-30, 4, (1983).
2. D.J. Clark, Y. Jongen, and C.M. Lyneis, Proceedings of the 10th Int'l Conf on Cyclotron and their Applications, pp. 133-136, E. Lansing, MI, (1984)
3. C.M. Lyneis and D.J. Clark, IEEE Trans. NS-32, 5, 1745 (1985)
4. C. Lyneis, Nucl. Instr. and Meth. in Phys. Res. B 10/11, 775 (1985)
5. C. M. Lyneis, Proc. 11th Int'l Cyclotron Conf., Tokyo, Oct.1986.
6. D. J. Clark and C. M. Lyneis, Proc. 11th Int'l Cyclotron Conf., Tokyo, Oct. 1986.

Table 1. Currents for the LBL ECR: Hydrogen through Silicon

| CS | $^{1}$H | $^{3}$He | $^{12}$C | $^{14}$N | $^{16}$O | $^{19}$F | $^{20}$Ne | $^{24}$Mg | $^{28}$Si |
|---|---|---|---|---|---|---|---|---|---|
| 1+ | 300 | 300 | 27 | 82 | 118 | | | | |
| 2+ | | 200 | 37 | 117 | 143 | 43 | 51 | 32 | 20 |
| 3+ | | | * | 106 | 152 | 55 | 63 | 34 | 33 |
| 4+ | | | 31 | 110 | * | 53 | 78 | 28 | 69 |
| 5+ | | | 6.5 | 93 | 96 | 37 | 58 | 44 | 72 |
| 6+ | | | | 19 | 82 | 17 | 45 | 34 | 47 |
| 7+ | | | | | 14 | 11 | 21 | 18 | 30 |
| 8+ | | | | | 0.95 | 1 | 11 | 8 | 17 |
| 9+ | | | | | | 0.05 | 1.1 | 6.3 | 7 |
| 10+ | | | | | | | 0.04 | 2.2 | 2.7 |
| 11+ | | | | | | | | 0.1 | 0.5 |
| 12+ | | | | | | | | | 0.2 |

All currents in eμA measured at 10 kV extraction voltage.

* Indicates not measured because a mixture of two ions with identical charge to mass ratios were present.

Natural isotopic abundance source feeds were used except for $^{3}$He. Cyclotron external beam was used to estimate ECR $^{16}O^{8+}$ current. ECR $^{22}Ne^{10+}$ current was used to estimate ECR $^{20}Ne^{10+}$ current.

Table 2. Currents for the LBL ECR: Sulfur through Xenon

| CS | $^{32}$S | $^{39}$K | $^{40}$Ar | $^{40}$Ca | $^{48}$Ti | $^{84}$Kr | $^{127}$I | $^{129}$Xe |
|---|---|---|---|---|---|---|---|---|
| 3+ | 10 | 4 | 38 | 23 | | | | |
| 4+ | * | 4.5 | 82 | 24 | | | | |
| 5+ | 20 | 5 | * | * | | | | |
| 6+ | * | 8.5 | 60 | 37 | | 9 | | |
| 7+ | 63 | 11 | 66 | 38 | 2.4 | 12 | | |
| 8+ | * | 18 | 106 | 36 | * | 22 | | |
| 9+ | 36 | 37 | 72 | 31 | 12 | 25 | | 4.1 |
| 10+ | * | 22 | * | * | 10 | 22 | 4.2 | 4.7 |
| 11+ | 5 | 12 | 18 | 22 | 8 | 19 | 4.9 | 5.1 |
| 12+ | * | 2.4 | 13 | 11 | * | * | 5.7 | 5.2 |
| 13+ | .4 | | 5 | 3.2 | 1 | 21 | 7.5 | 5.2 |
| 14+ | * | | 1.4 | 1.1 | | * | 8.5 | 5 |
| 15+ | .001 | | * | * | | 16 | 11 | 4.3 |
| 16+ | | | 0.03 | 0.03 | | 8 | * | 4.6 |
| 17+ | | | | | | 7 | 12 | 4.3 |
| 18+ | | | | | | * | 15 | 4.4 |
| 19+ | | | | | | 2 | 15 | 4.8 |
| 20+ | | | | | | 0.9 | 14 | 4.8 |
| 21+ | | | | | | * | * | 4 |
| 22+ | | | | | | 0.1 | 11 | 3.5 |
| 23+ | | | | | | | 10 | 3.1 |
| 24+ | | | | | | | 8.3 | 2.7 |
| 25+ | | | | | | | 5.6 | 2 |
| 26+ | | | | | | | 2.1 | 1.1 |
| 27+ | | | | | | | 0.83 | 0.34 |
| 28+ | | | | | | | 0.2 | |
| 29+ | | | | | | | 0.05 | |
| 30+ | | | | | | | 0.009 | |

All currents in eμA measured at 10 kV extraction voltage.

* Indicates not measured because a mixture of two ions with identical charge to mass ratios were present.

Natural isotopic abundance source feeds were used.

Table 3. Some Optimized Beams

| Ion | Cyclotron Energy (MeV) | Harm. | Source Current (eμA) | Cyclotron External Current (eμA) | Transmission (%) |
|---|---|---|---|---|---|
| $^{14}N^{5+}$ | 180 | 1 | 60 | 7 | 11 |
| $^{16}O^{2+}$ | 20 | 3 | 69 | 2 | 3 |
| $^{16}O^{2+}$ | 20 | 5 | 67 | .15 | .2 |
| $^{18}O^{5+}$ | 117 | 1 | 60 | 10 | 17 |
| $^{16}O^{6+}$ | 315 | 1 | 40 | 3 | 7 |
| $^{16}O^{7+}$ | 429 | 1 | 10 | .2 | 2 |
| $^{22}Ne^{6+}$ | 151 | 1 | 40 | 7 | 17 |
| $^{24}Mg^{7+}$ | 192 | 1 | 20 | 1.5 | 7 |
| $^{28}Si^{6+}$ | 180 | 1 | 60 | 3 | 5 |
| $^{40}Ar^{9+}$ | 180 | 3 | 30 | 3 | 10 |
| $^{40}Ar^{12+}$ | 504 | 1 | 6 | .2 | 3 |
| $^{86}Kr^{14+}$ | 301 | 3 | 2.5 | .08 | 3 |
| $^{129}Xe^{21+}$ | 451 | 3 | .8 | .02 | 3 |

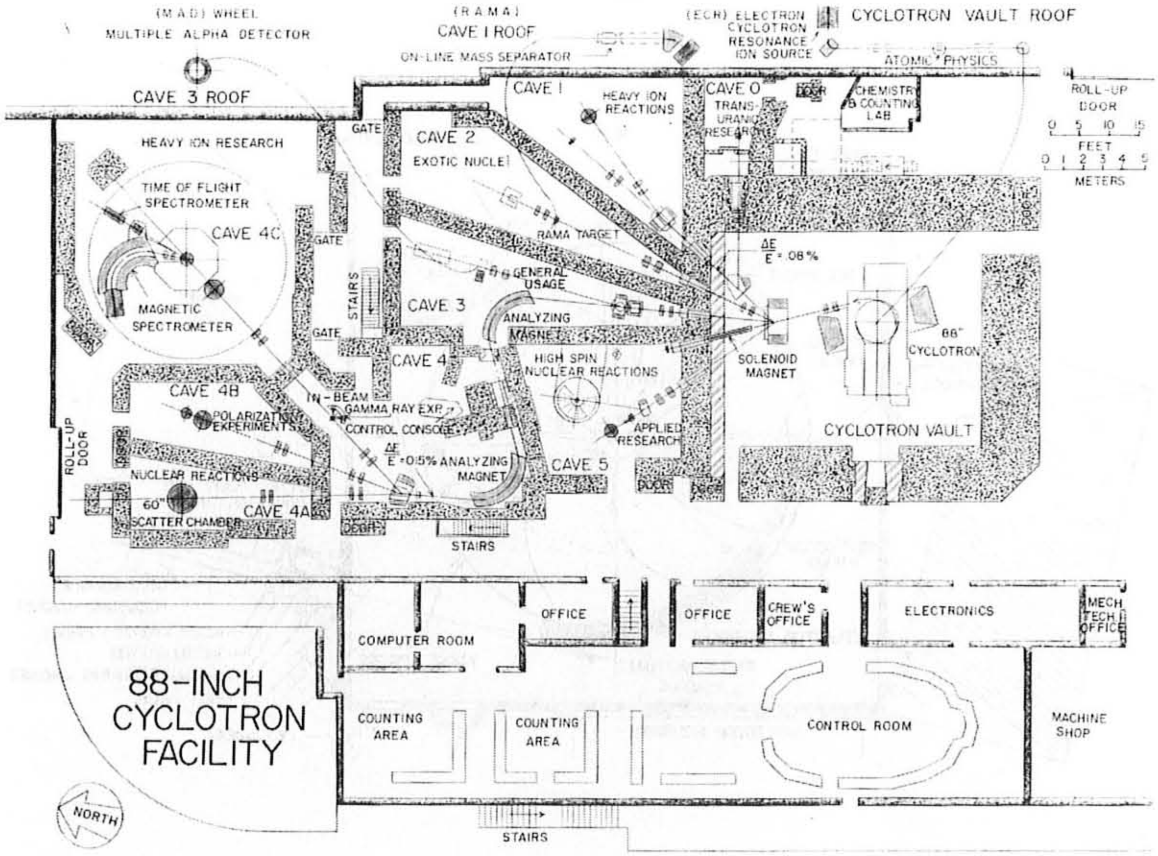

Fig. 1. LBL 88-Inch Cyclotron and Experimental Caves. CBB 8610-8005

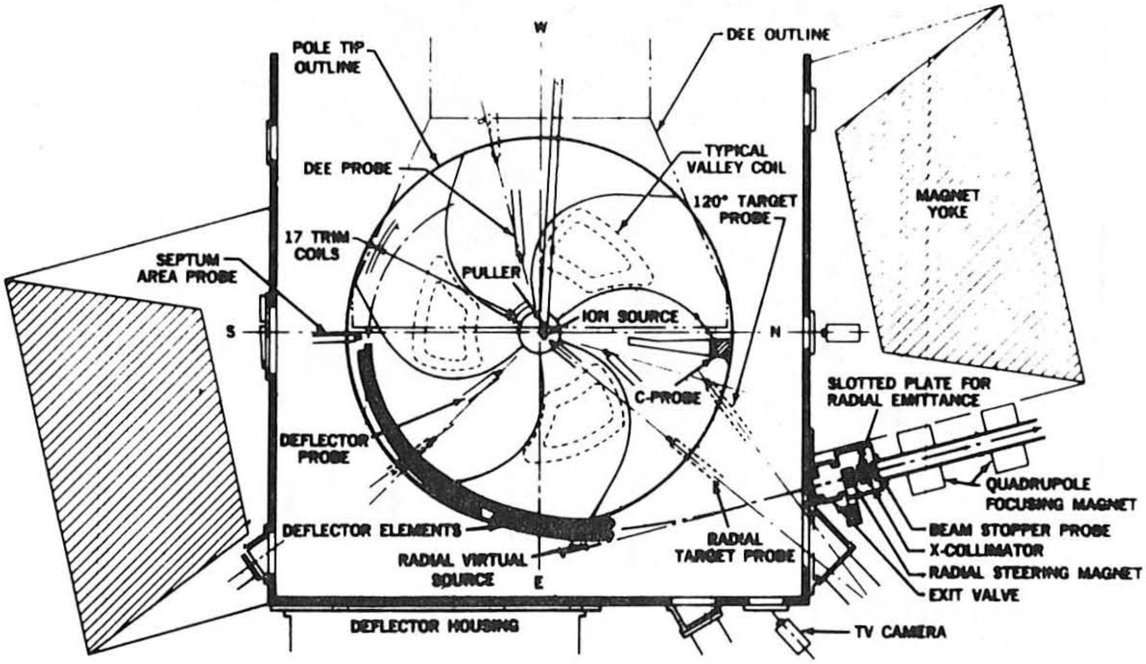

Fig. 2. Plan view of cyclotron at midplane. XBL 678-4699

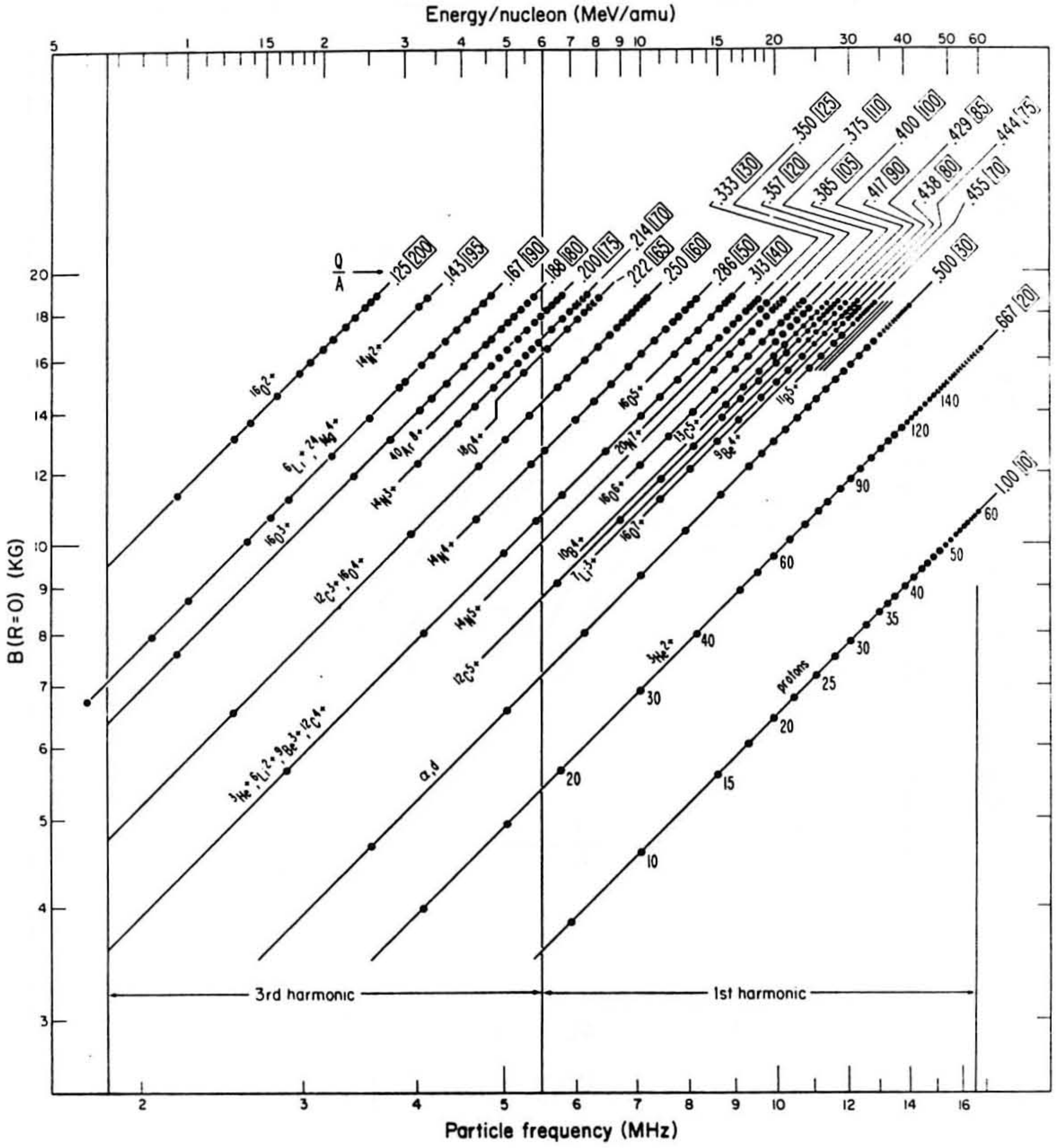

Fig. 3. Cyclotron resonance chart for many ions.

XBL 811-62

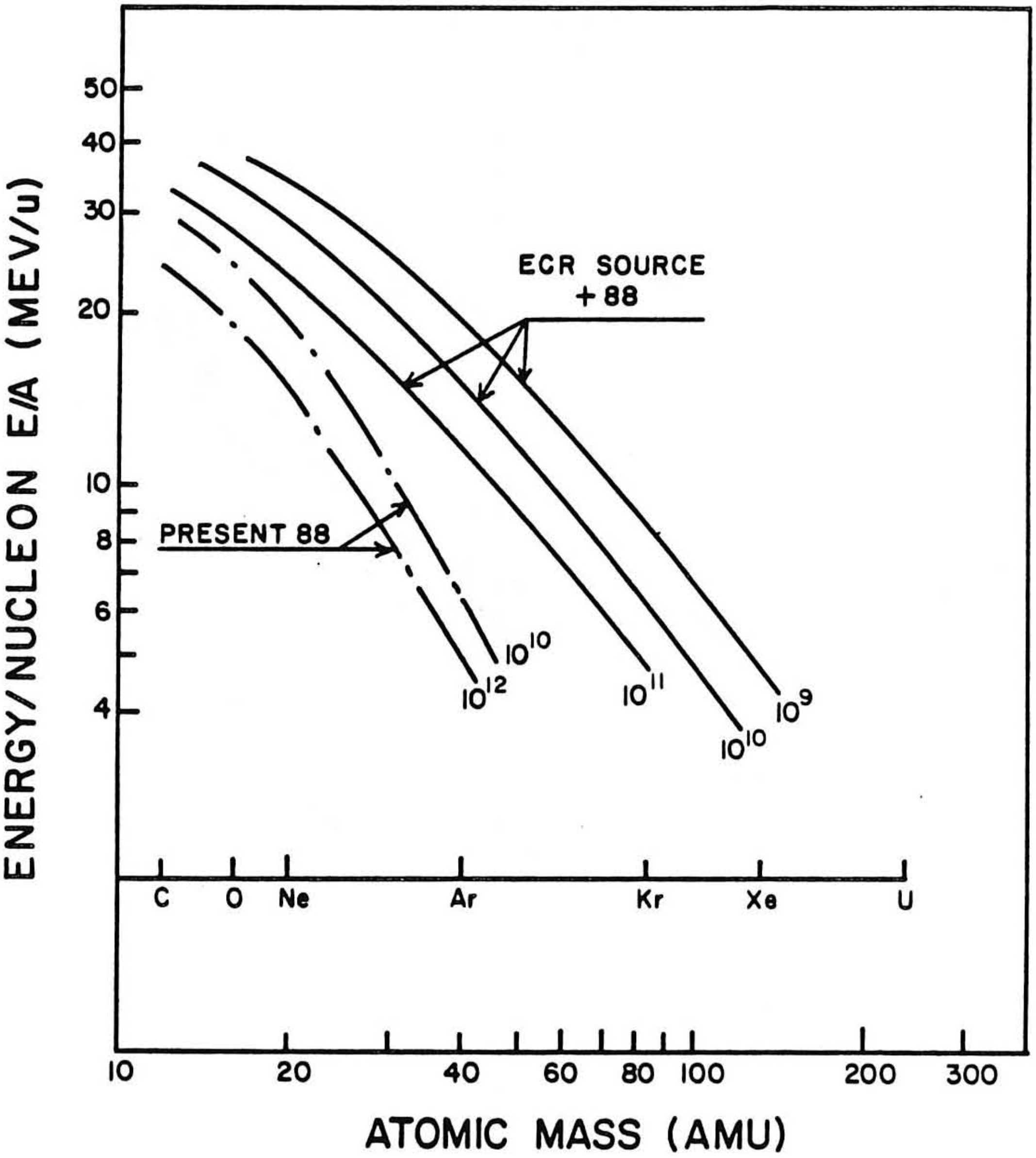

Fig. 4. Intensity contours in particles/sec for operation with internal PIG source (PRESENT 88) and external ECR source. XBL 833-8746

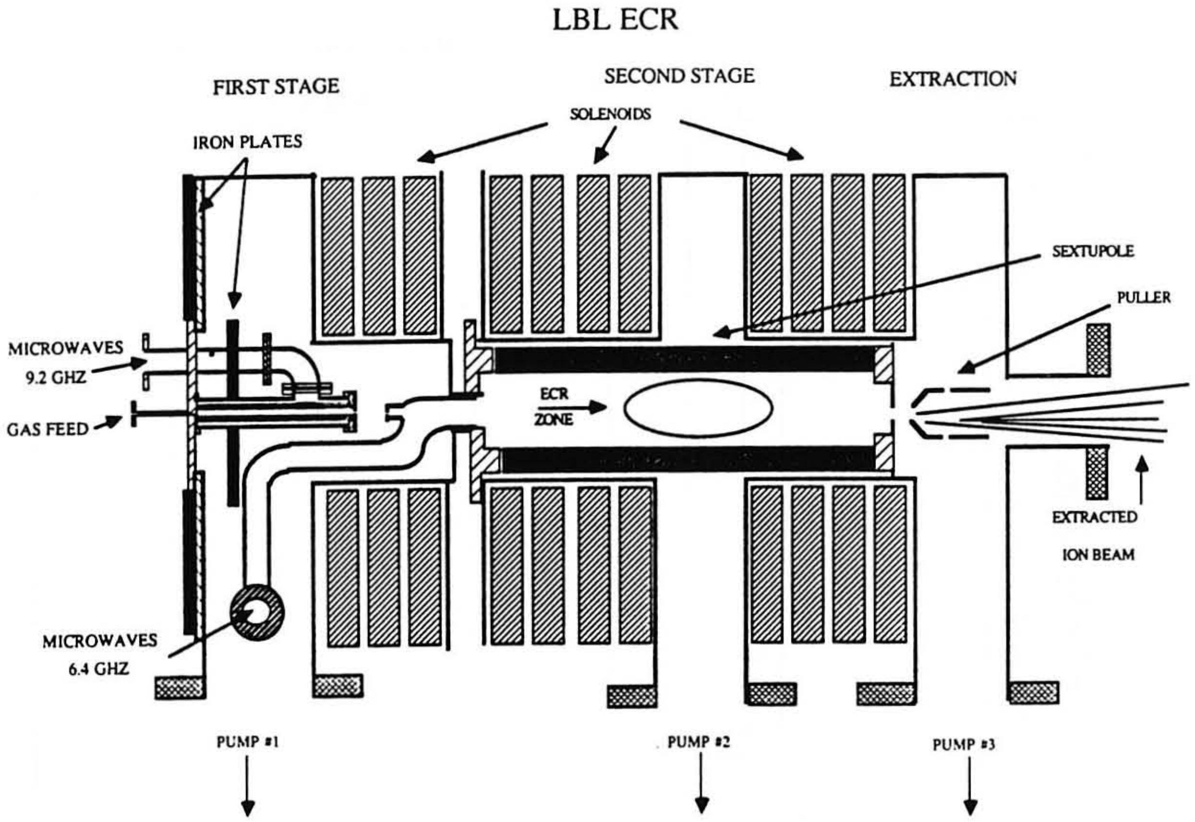

Fig. 5. Schematic cross-section of ECR source. XBL 867-2602

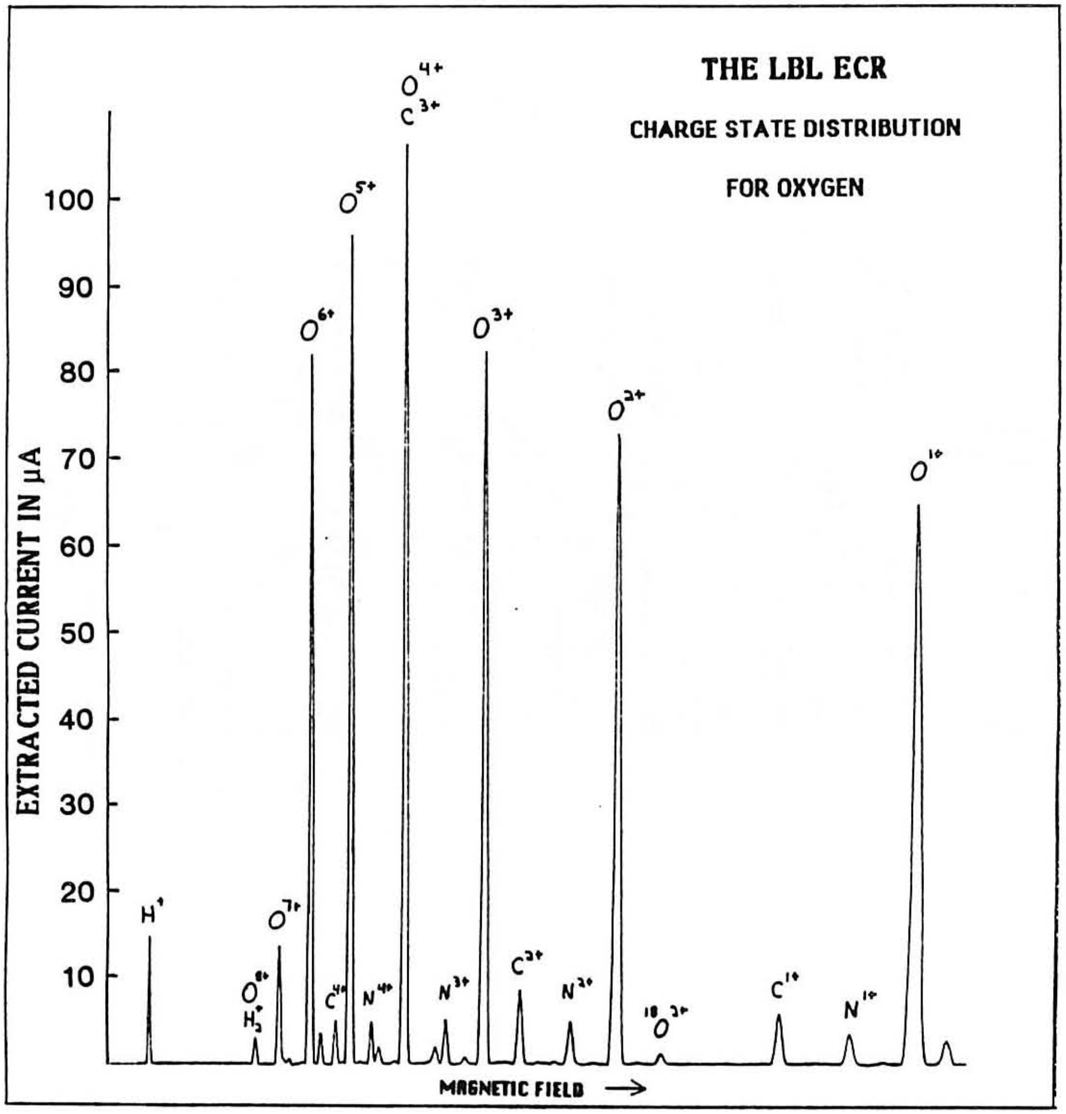

Fig. 6. Charge state distribution for oxygen, tuned for $O^{7+}$. The analyzing magnet field was swept.

XBL 8611-4412

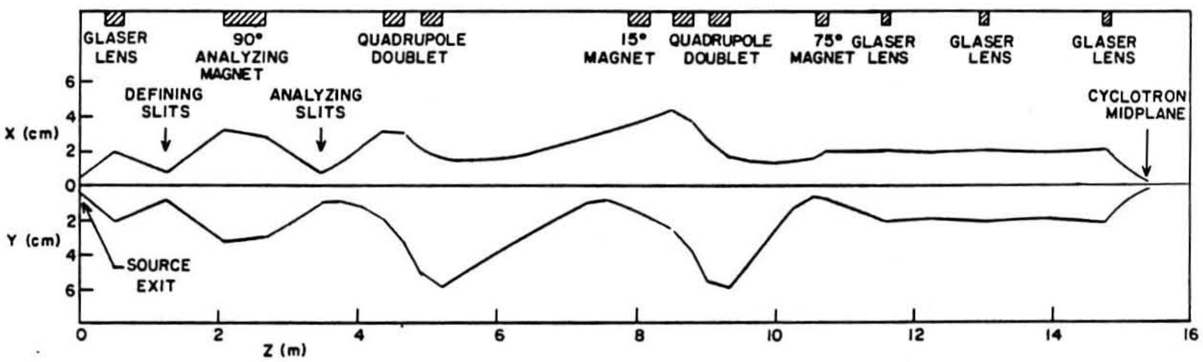

Fig. 7. Beam envelope (1/2 width) calculation in horizontal and vertical planes from ECR source to cyclotron midplane. XBL 845-1775

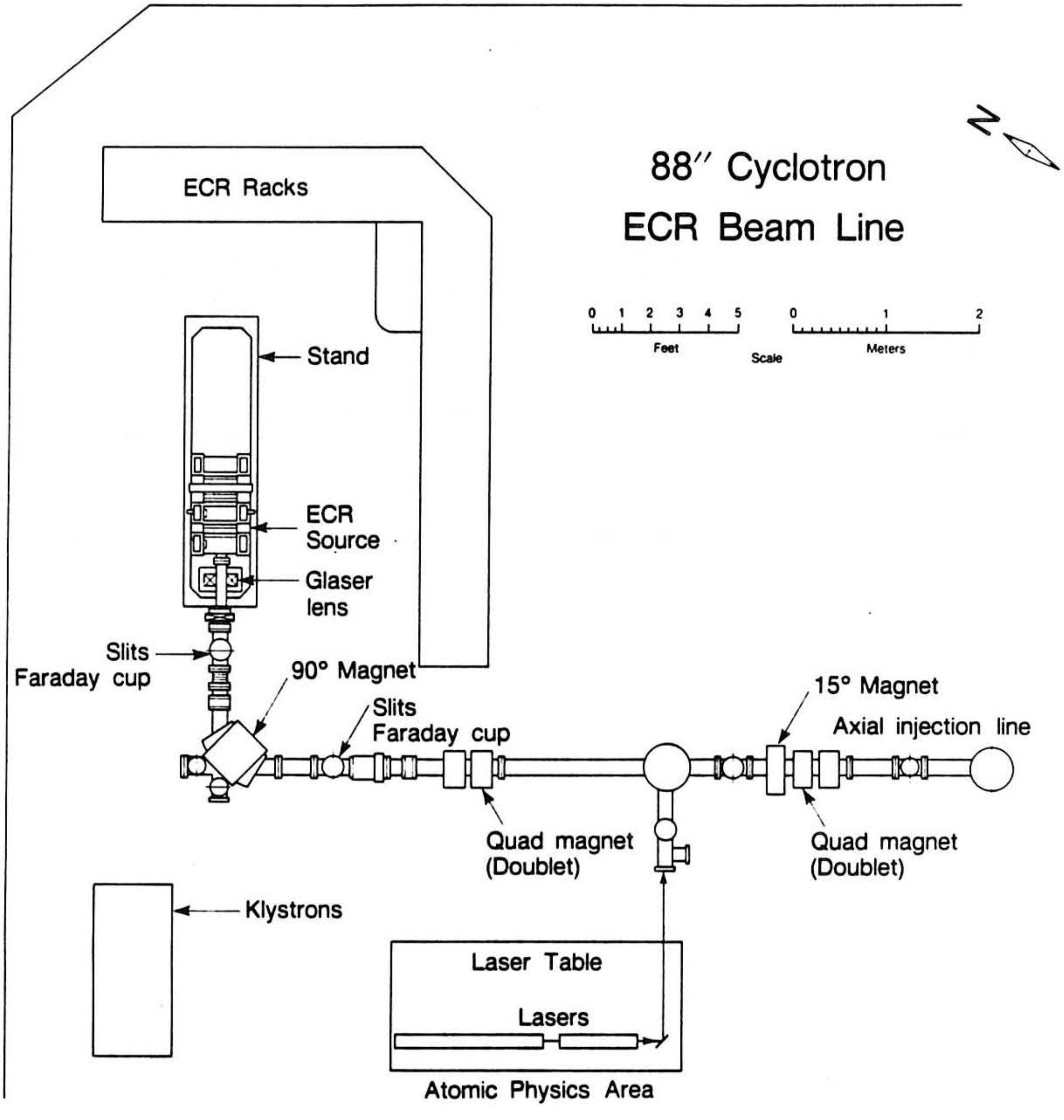

Fig. 8. ECR Source and horizontal section of injection line. XBL 863-921

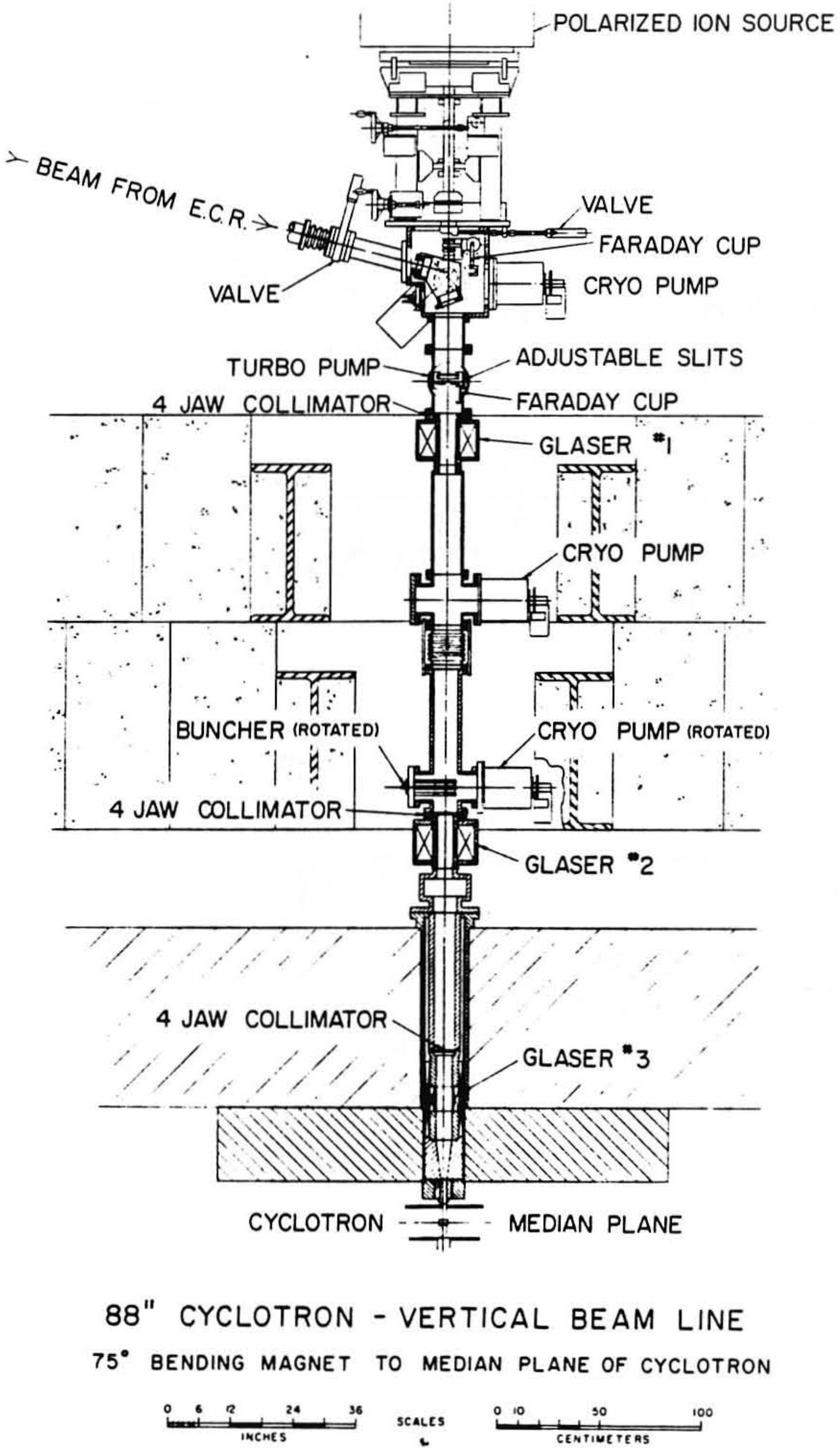

Fig. 9. Vertical section of injection line.

XBL 8610-3630

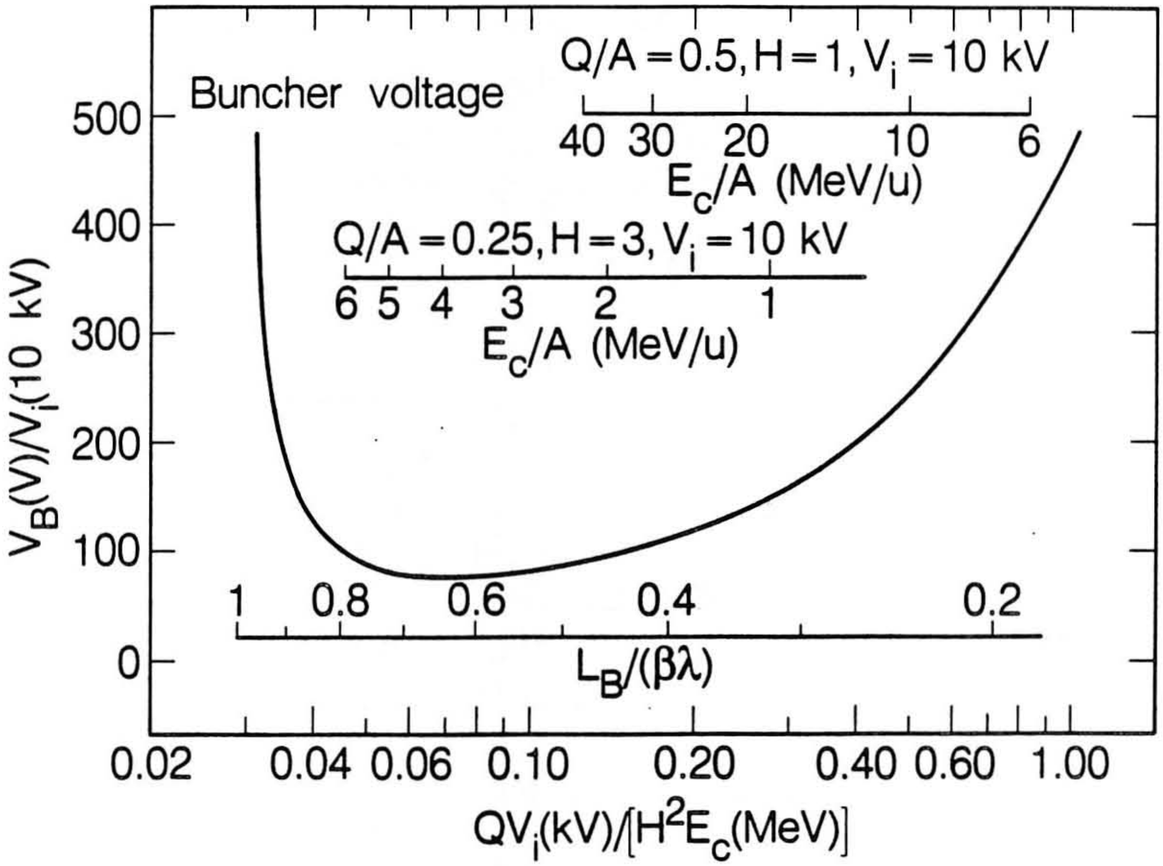

Fig. 10. Buncher voltage as a function of cyclotron parameters. XBL 8610-12041

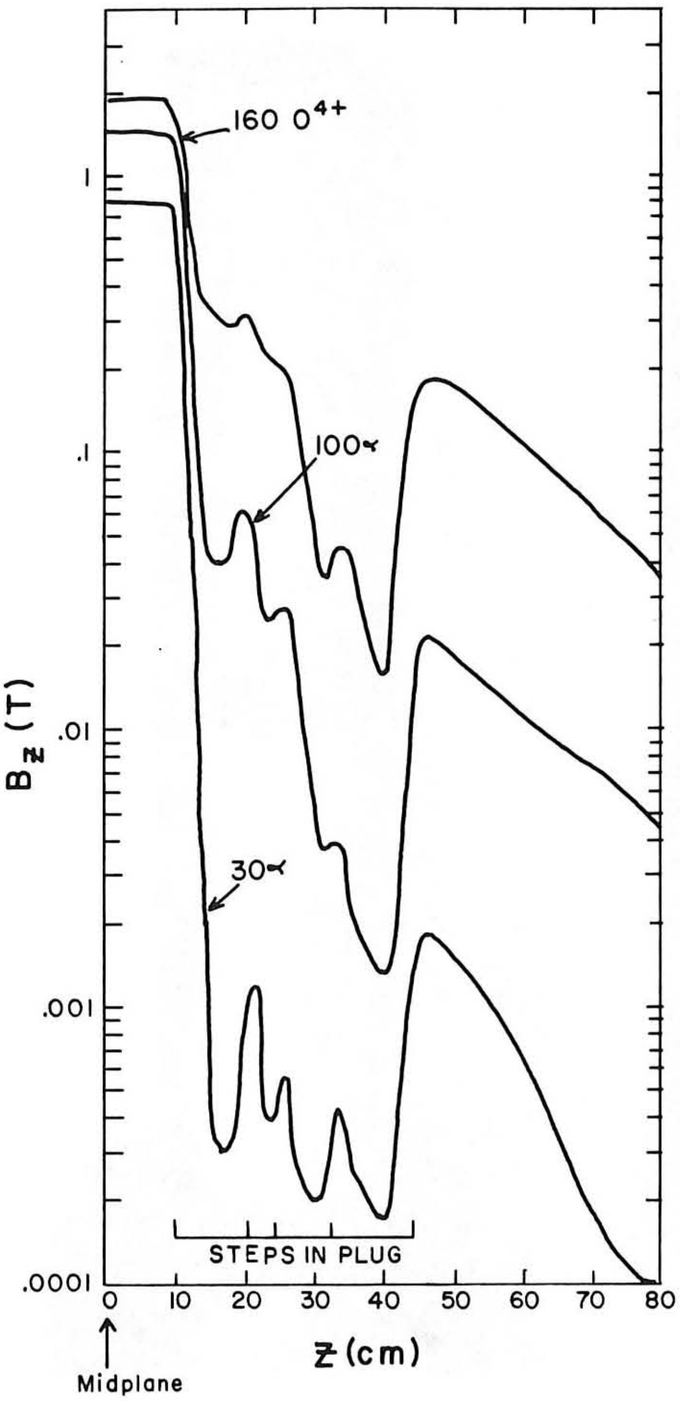

Fig. 11. Axial magnetic field measurement from midplane up cyclotron pole axis for 3 field levels. XBL 833-8752

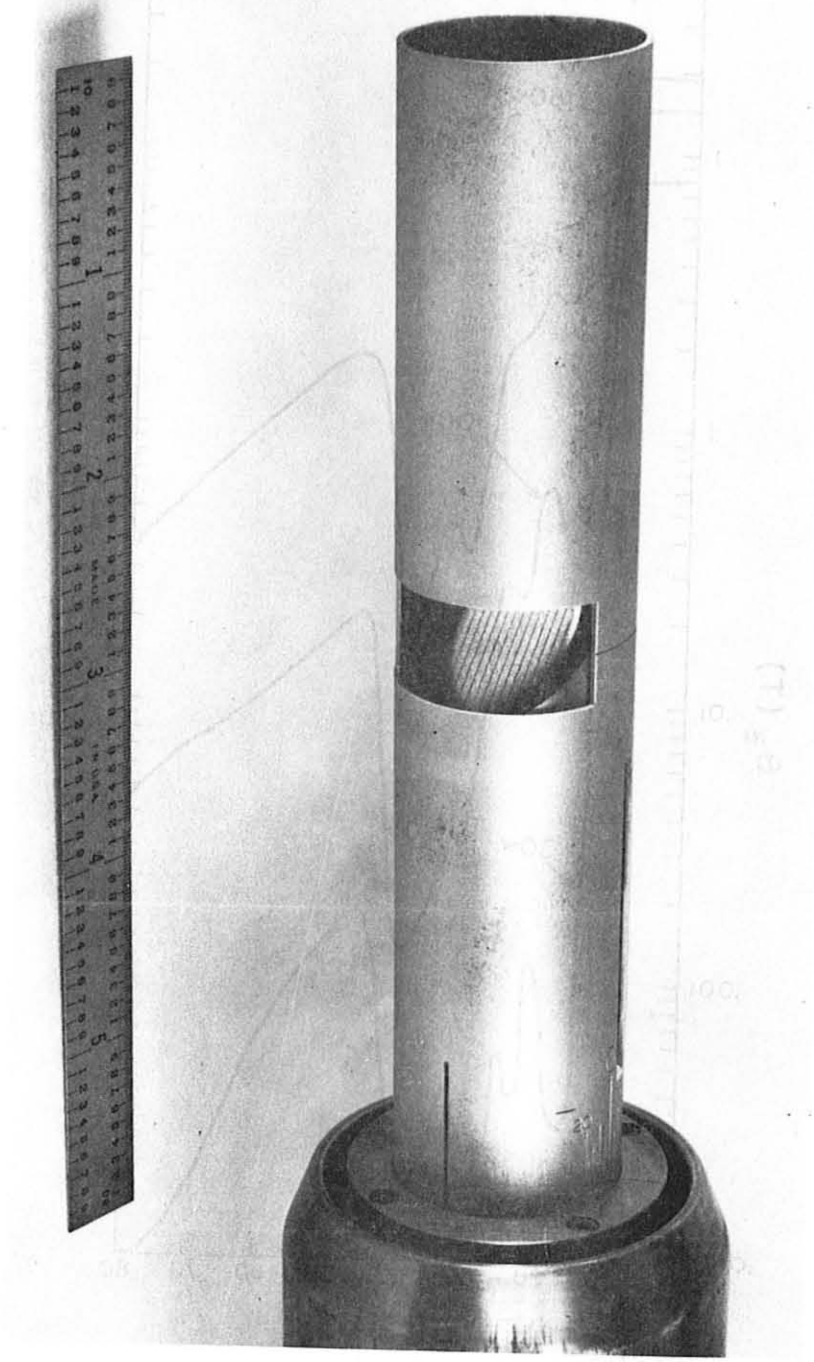

Fig. 12. Electrostatic gridded mirror in housing. CBB 869-7625

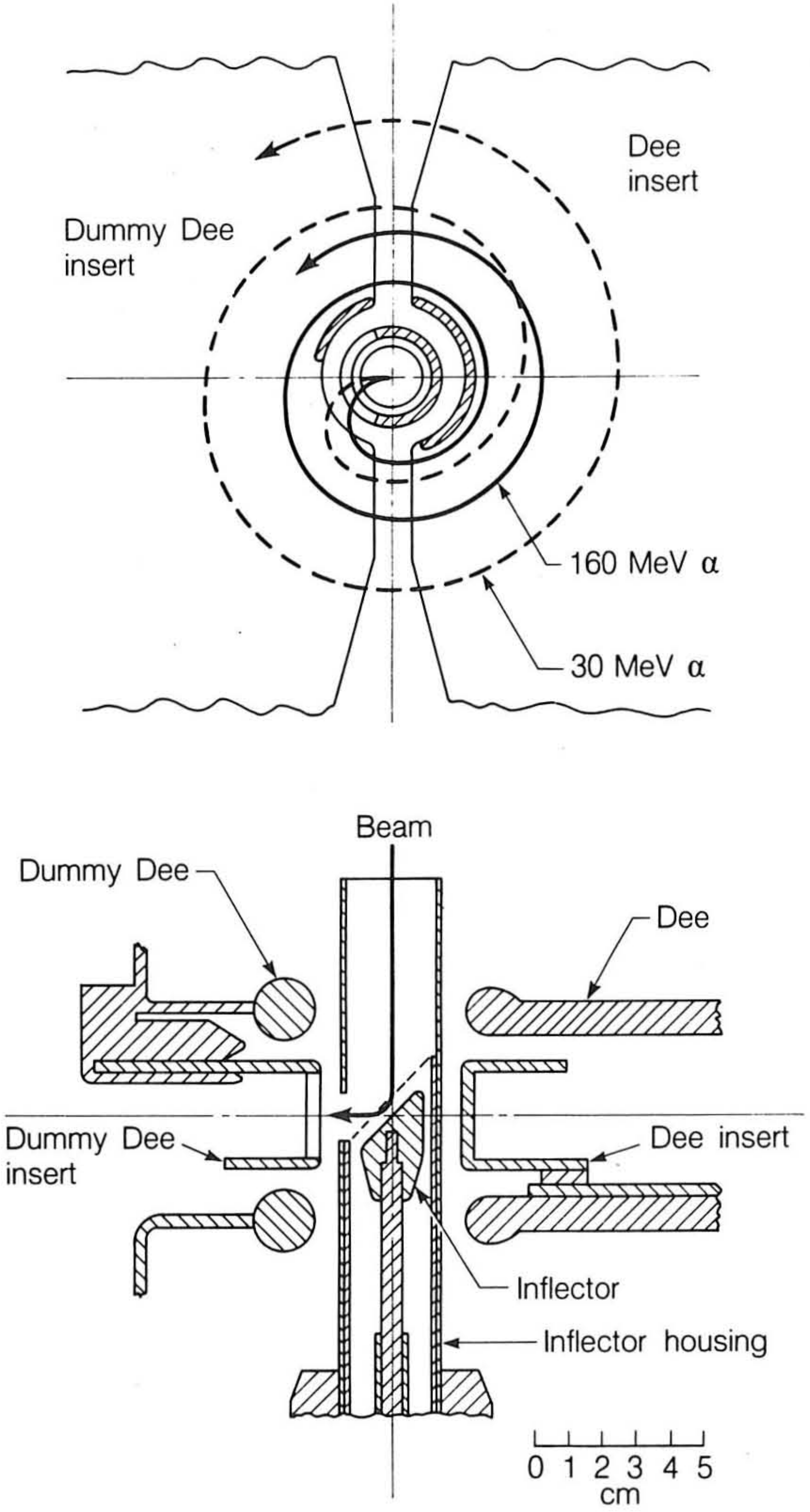

Fig. 13. Central region of cyclotron in plan and elevation views. XBL 8610-12042